Controlling graphene corrugation on lattice-mismatched substrates

A. B. Preobrajenski,[1,*] May Ling Ng,[1,2] A. S. Vinogradov,[3] and N. Mårtensson[1,2]
[1]*MAX-Laboratory, Lund University, Box 118, 22100 Lund, Sweden*
[2]*Department of Physics, Uppsala University, Box 530, 75121 Uppsala, Sweden*
[3]*V. A. Fock Institute of Physics, St.-Petersburg State University, 198504 St.-Petersburg, Russia*
(Received 10 July 2008; published 4 August 2008)

By means of synchrotron-radiation-based core-level spectroscopies we demonstrate that the degree of corrugation in graphene nanomesh on lattice-mismatched transition-metal substrates critically depends on the strength of chemical bonding at the interface. The degree of interfacial orbital hybridization between graphene and metal states is rising in the series Pt(111)-Ir(111)-Rh(111)-Ru(0001). This growing strength of hybridization is accompanied by a gradual change in graphene morphology from nearly flat to strongly corrugated. We provide a comparison of the pore size and period for the cases of graphene and *h*-BN nanomesh on Rh(111).

DOI: 10.1103/PhysRevB.78.073401 PACS number(s): 68.43.−h, 68.65.Cd, 78.70.Dm, 79.60.Jv

Self-assembly of atoms and molecules on atomically well-defined surfaces becomes an increasingly attractive route to mass production in modern nanotechnology due to the ease of fabrication and good control over the size, shape, and lateral distribution of the resulting nanostructures.[1] One of the most fascinating and technologically promising ways toward mass production of well-ordered quantum dot assemblies in two dimensions is based on the use of self-assembled templates from layered materials, e.g., graphite and hexagonal boron nitride (*h*-BN).[2–7] These templates (often called "nanomesh") represent highly perfect monatomic layers of graphite or *h*-BN, considerably corrugated with a period of several nanometers. The most prominent examples of such templates are *h*-BN nanomeshes on Rh(111) (Refs. 4, 8, and 9) and Ru(0001).[5] The *h*-BN nanomesh can be prepared by thermal decomposition of vaporized borazine on a transition-metal (TM) substrate with threefold or sixfold symmetry and suitable (a few percent) lattice mismatch to *h*-BN. However, a significant corrugation of the *h*-BN monolayer can be obtained only at interfaces with considerable orbital mixing between TM *d* states and *h*-BN π states, resulting in considerable covalent bonding.[10] Thus, while the period of the *h*-BN nanomesh is determined by the lattice mismatch, the diameter and the depth of the nanomesh pores depend on the strength of interfacial bonding.[11]

As regards monolayer graphite (MG) (or graphene), despite decades of intense studies of its adsorption on TM substrates, there is a lack of systematic information about the structure and chemistry of graphitic nanotemplates based on lattice-mismatched MG/TM interfaces. Only recently, atomically resolved scanning tunneling microscopy (STM) studies of MG on Ir(111) (Ref. 3) and Ru(0001) (Ref. 12) have demonstrated that single-domain moiré patterns with very high degree of structural perfection and periodicity of ~3 nm can be formed, thus being very promising as templates for nanotechnology. Moreover, an unusually high STM contrast was observed at the MG/Ru(0001) interface, which was associated with possibly stronger chemical bonding as compared to other mismatched MG/TM interfaces.[12] Therefore, it is plausible to suggest that there is a dependence between the strength of chemical interaction and the degree of graphene corrugation at the mismatched MG/TM interfaces, much as in the *h*-BN/TM systems.[11] The validity of this assumption can be verified by spectroscopic techniques since they yield direct information about the strength of interfacial chemical bonds.

In this Brief Report we present a systematic study of chemical versus structural effects at the MG/Pt(111), MG/Ir(111), MG/Rh(111), and MG/Ru(0001) interfaces using near-edge x-ray absorption fine structure (NEXAFS) and photoelectron spectroscopy (PES). We report on the observed correlation between chemical bonding at the lattice-mismatched MG/TM interfaces and the corrugation of graphene. Furthermore, we propose a clear definition to the concept of "graphene nanomesh" and compare its structure with that of the *h*-BN nanomesh.

The experiments were carried out at beamline D1011 at MAX-Laboratory (Lund, Sweden) with a photon energy resolution of 80 meV at the C *K* edge and a total-energy resolution of 150 meV for the C 1*s* PE spectra. The NEXAFS spectra were recorded in the partial electron yield mode (repulsive potential $U=-100$ V) by a multichannel-plate detector and normalized to the background curves recorded in the same mode from the same substrates but without graphene. The base pressure during the measurements did not exceed 2×10^{-10} mbar.

Substrates were cleaned by repeated cycles of Ar^+ sputtering, annealing in oxygen ($p=5\times10^{-8}$ mbar at $T\sim900-1100$ K), and subsequent flashing in UHV to 1400 K. Graphene was prepared by thermal decomposition of propene gas at $T=920$ K for all substrates. In order to reduce the nucleation rate and the density of grain boundaries we preserved low propene pressure [$(2-3)\times10^{-8}$ mbar] and used long preparation time (up to 1 h) to ensure saturated coverage. The formation of exactly one graphite monolayer (no multilayers) was confirmed by PES. The reference highly oriented pyrolytic graphite (HOPG) sample was cleaved in UHV.

The C 1*s* NEXAFS spectra for all studied interfaces are compared in Fig. 1 along with the corresponding low-energy electron-diffraction (LEED) patterns. In the reference HOPG spectrum peaks A, B, and C result from the promotion of core electrons into π^*, σ_1^*, and σ_2^* orbitals, respectively, with essential influence of excitonic effects (poor core-hole screening) on the shape of peaks A and B.[13,14] In going from HOPG to MG/Pt(111) the overall spectral shape remains nearly unchanged, thus indicating a lack of orbital hybridization between carbon and platinum states. This results in a

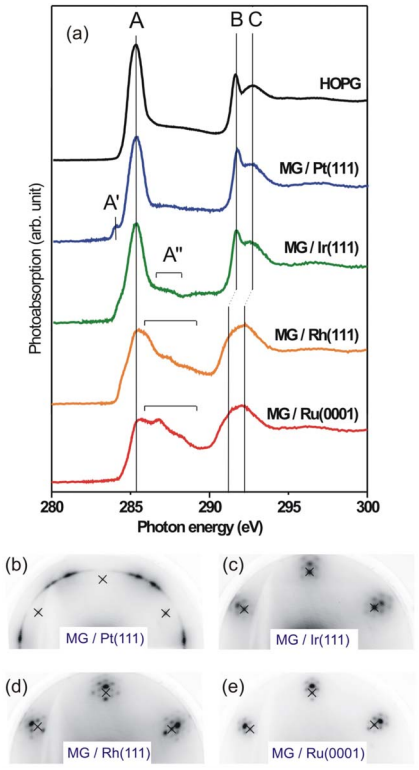

FIG. 1. (Color online) (a) C 1*s* NEXAFS spectra from monolayer graphite adsorbed on several lattice-mismatched TM surfaces. The C 1*s* spectrum from HOPG is shown for comparison. [(b)–(e)] Corresponding LEED patterns (E=60 eV); substrate-related spots are marked with crosses.

very weak chemical bonding of graphene to Pt(111), which is even not strong enough to uniquely force the overlayer in registry with the substrate, as can be judged from the incommensurate structure in the LEED pattern [Fig. 1(b)]. Similar LEED patterns were observed in the earlier studies,[15,16] indicating a variety of preferred orientations, as proved later by observation of a variety of moirélike superstructures in STM.[17–19] The only difference in the C 1*s* NEXAFS of MG/Pt(111) as compared to bulk graphite is the emergence of weak shoulder A′ at ~284 eV. This shoulder was observed before for graphite and carbon nanotubes intercalated with $FeCl_3$ and associated with the lowering of the Fermi level (E_F) induced by the charge transfer.[20,21] Besides, weak orbital mixing may contribute to some modification of the bulk band structure in the vicinity of E_F. The latter effect becomes more important for interfaces with stronger chemical bonding.

Small but visible changes occur further in going to the C 1*s* NEXAFS in the MG/Ir(111) system [Fig. 1(a)]. Here shoulder A′ is growing in relative intensity, and a new feature (denoted A″) starts to appear in the energy range between the π^* and σ_1^* resonances, thus indicating some (though weak) increase in the degree of orbital mixing in comparison with the MG/Pt interface. This increase is reflected also in the coincidence lattice structure with just one single domain observed in LEED [Fig. 1(c)]. A reduction in the 5*d* occupancy in going from Pt (d^9) to Ir (d^7) is probably the main reason for the growing covalent bonding (5*d* shell contribution to the bonds is higher for Ir). In general, however, the bonding of graphene to the 5*d* metal surfaces is weak.

In going from 5*d* (Ir, Pt) to 4*d* (Rh, Ru) metals the C 1*s* NEXAFS spectrum of adsorbed graphene changes drastically indicating strong chemisorption [Fig. 1(a)]. The π^*-derived band A′ can now be associated mainly with the continuum of the hybridization-induced gap states of graphene, similar to the states recently observed for monolayer *h*-BN on TM surfaces.[22] Not only the chemisorption-induced π^* bands A′ and A″ continue to develop but also the σ^* bands. Indeed, the entire σ^* manifold is shifted by ~0.5 eV to lower photon energies, and the σ_1^* resonance is smeared out into a shoulder. A reduction in the π-σ energy separation is a signature of the π bond softening in graphene on Rh(111) and Ru(0001) due to the electron sharing with the substrates. Similar effects were observed by other techniques in graphene chemisorbed on TM carbides[23] and Ni(111).[24] A broadening of the σ_1^* resonance is another evidence for a strong orbital hybridization and electron sharing at the MG/Rh and MG/Ru interfaces because it indicates strong delocalization of the corresponding core-excited state. The overall spectral variation of the C 1*s* NEXAFS indicates a growing strength of covalent interfacial bonding from top to bottom in Fig. 1(a). Very similar variations were observed in the B 1*s* NEXAFS spectra of *h*-BN monolayers on the same TM substrates with the degree of orbital hybridization growing in the same sequence.[10,11]

Although the covalent bonding at the MG/Rh and MG/Ru interfaces is significantly stronger than at MG/Ir, all three systems show similar moirélike patterns in LEED due to similar lattice mismatch [Figs. 1(c)–1(e)] and cannot be really distinguished without an *I*-*V* curve analysis. However, the C 1*s* PES can help in revealing possible variations in graphene morphology. In Fig. 2 we show the C 1*s* spectra for HOPG and all four interfaces under study, along with the results of our peak-fit analysis. The parameters used for the peak fits are summarized in Table I.

At this point it is necessary to note that for the MG/Ru(0001) system we had to subtract the Ru $3d_{3/2}$ signal at 284.2 eV, which was almost coinciding with C 1*s*. This procedure is not trivial and should be explained below in some detail because Ru 3*d* line shape is also modified by the interaction with MG, thus being unknown *a priori*. First, we fitted the Ru 3*d* doublet from clean Ru(0001) into surface- and bulk-related doublets, as shown in Fig. 3(a). Then we fitted Ru 3*d* in MG/Ru with several of these (bulk-related) functions until rather flat residual intensity was observed after subtraction in the region of Ru $3d_{5/2}$ at 280.0 eV [Fig. 3(b)]. A complete subtraction of the $3d_{5/2}$ component of the Ru 3*d* doublet automatically results also in a complete subtraction of the second ($3d_{3/2}$) component. Finally, we checked that the C 1*s* line shape for MG/Ru presented in Fig. 2 is correct by measuring this spectrum with lower photon energy, thus reducing the Ru 3*d* contribution [Fig. 3(c)]. The double-peak shape of the C 1*s* signal is evident in this case even without any spectrum modification.

The C 1*s* photoelectron spectrum of HOPG (Fig. 2) contains only one component with the Lorentzian full width at half maximum (LFWHM) of 150 meV, in good agreement

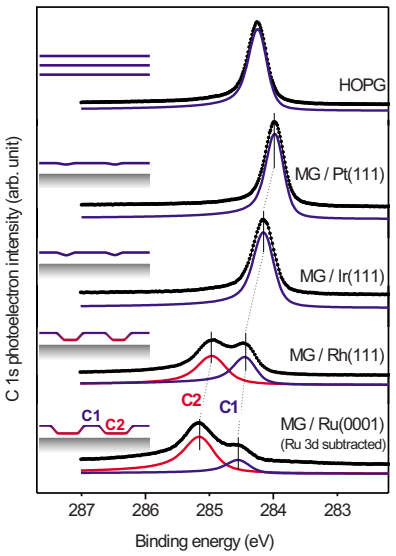

FIG. 2. (Color online) C 1*s* photoelectron spectra taken in normal emission from monolayer graphite adsorbed on several lattice-mismatched TM surfaces. Photon energy is 400 eV. For MG/Ru(0001) the Ru 3*d* signal is subtracted (see text and Fig. 3). The C 1*s* photoelectron spectrum from HOPG is shown for comparison. Schematics illustrate resulting graphene morphology.

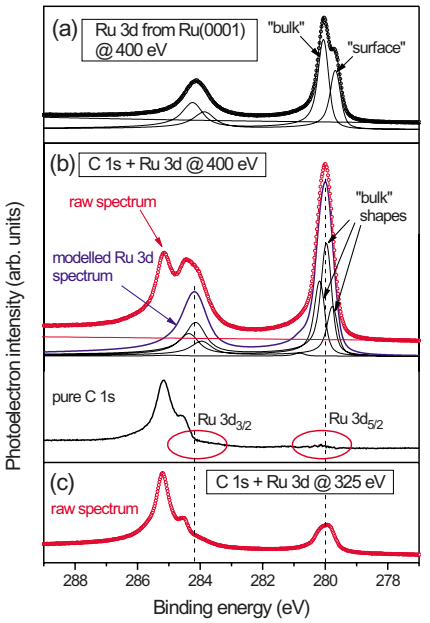

FIG. 3. (Color online) (a) Ru 3*d* PES from clean Ru(0001) excited with $h\nu$=400 eV and decomposed in surface-related and bulk-related contributions; (b) "raw" C 1*s* and Ru 3*d* spectrum from MG/Ru(0001) excited with $h\nu$=400 eV fitted with several "bulk" Ru 3*d* shapes to model the substrate contribution (the result of subtraction is shown below); (c) raw C 1*s* and Ru 3*d* spectrum from MG/Ru(0001) excited with $h\nu$=325 eV.

with earlier studies.[25,26] For graphene on Pt(111) and Ir(111) the C 1*s* line is also single with the LFWHMs of 130 and 150 meV, respectively. Such a low value for the LFWHM from MG/Pt is probably natural for an almost ideal "levitating" graphene, while in HOPG it may be broadened by defects.[26] For MG/Ir both the total and the Lorentzian widths are slightly larger than at MG/Pt as a consequence of increased orbital mixing. In going to MG/Rh and MG/Ru, the C 1*s* line becomes split in two distinct components with energy separations of 0.53 and 0.60 eV on Rh and Ru, respectively. We associate this double-peak shape with a significant corrugation of graphene, as illustrated schematically in Fig. 2. The component with lower binding energy (C1) is due to the elevated (nonbonding) parts of the graphene sheet, while the high-energy peak (C2) results from the strongly bonded parts. This assignment is justified by evidently larger Lorentzian widths of C2 (300–330 meV) as compared to C1 (160 meV) and growing relative intensity of C2 in going from MG/Rh to more reactive MG/Ru. Rather large LFWHM of C2 mainly simulates the effect of gradually varying chemical surrounding of the C atoms inside the pores, but in part it may be also due to the shorter lifetime of the core-ionized states caused by chemisorption. Note that in the N 1*s* photoelectron spectrum of *h*-BN adsorbed on the same TM substrates similar two components, N1 and N2, were observed and assigned to the wires and pores of the *h*-BN nanomesh,

TABLE I. Fit parameters (in eV, except α) for the C 1*s* spectra from Fig. 2 fitted with Doniach-Sunjic profiles (γ is the Lorentzian FWHM, α is the asymmetry parameter, and σ is the Gaussian FWHM). "B" stands for bonding and "NB" for nonbonding.

	E_B	FWHM	γ	α	σ
HOPG	284.23	0.35	0.15	0.10	0.23
MG/Pt(111)B					
NB	283.97	0.34	0.13	0.09	0.24
MG/Ir(111)B					
NB	284.16	0.40	0.15	0.10	0.27
MG/Rh(111)B	284.94	0.56	0.30	0.10	0.32
NB	284.41	0.46	0.16	0.18	0.29
MG/Ru(0001)B	285.12	0.61	0.33	0.15	0.30
NB	284.52	0.48	0.16	0.18	0.30

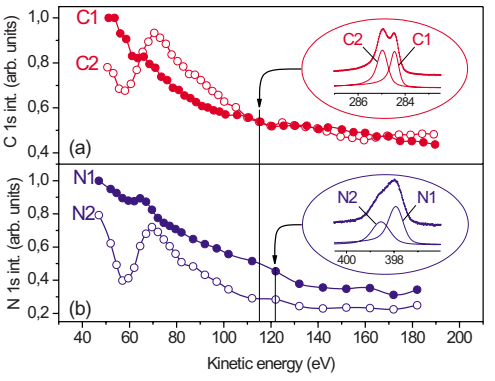

FIG. 4. (Color online) (a) Intensity evolution of C1 and C2 components of the C 1*s* photoelectron spectrum from graphene nanomesh on Rh(111) as a function of kinetic energy; (b) the same for N1 and N2 components of the N 1*s* spectrum from *h*-BN nanomesh on Rh(111) (from Ref. 10). All PES measurements performed at normal emission.

respectively.[11] In principle, it is plausible to define the concept of "nanomesh" for graphene (and also *h*-BN) on the basis of core-level PES: only those monolayers which show two strictly different chemical surroundings (i.e., two components in the core-level spectra) should be called by this term. In this sense, only MG/Rh and MG/Ru, but not MG/Pt and MG/Ir, can be considered as "true" nanomeshes, as visible from Fig. 2, where only two last spectra show two components each due to the pores (C2) and wires (C1) of the corrugated graphene. It is well known that the substrate-adsorbate distance for MG on TM surfaces depends on the chemical bonding. For instance, for the strongly bonded MG/Ni(111) interface the spacing between MG and the topmost Ni layer is only 2.1 Å,[27] much smaller than at the weakly bonded MG/Pt(111) interface [3.7 Å (Ref. 16)]. Therefore, we assume that the corrugation induced by strong chemical bonding is significant. In contrast, only weak corrugation of graphene is possible on Pt(111), as can be judged from the chemical inertness of the corresponding interface. For the MG/Ir(111) interface the corrugation should be slightly more pronounced (up to 0.27 Å, as calculated by N'Diaye *et al.*[3]).

It is interesting to compare the structure of *h*-BN and graphene nanomeshes on one and the same substrate. An insight in the structure can be gained on the basis of photoelectron diffraction (PED) data. In Fig. 4 we present a comparison of the C 1*s* and N 1*s* PED curves measured at normal emission as a function of kinetic energy from the MG/Rh(111) and *h*-BN/Rh(111) interfaces. Individual curves are obtained for the two components of each spectrum by a consistent peak-fit analysis of experimental data. It is remarkable that the PED curves from the corresponding components (pairs C1-N1 and C2-N2) are similar even in minor details, providing an evidence for considerable structural similarity between graphene and *h*-BN nanomeshes. However, the intensity ratio C1/C2 is systematically smaller than N1/N2 for all kinetic energies. The average values are 0.98 ± 0.15 for C1/C2 and 1.50 ± 0.25 for N1/N2. For the graphene nanomesh this implies either larger pores or smaller period of the pores as compared to *h*-BN/Rh(111). Based on the analysis of the moiré pattern in LEED for MG/Rh(111) we find the MG-to-Rh cell ratio very close to 12:11, resulting in the moiré pattern periodicity of 2.96 nm. With this parameter the calculated radius of the pore is 1.10 ± 0.05 nm, very close to the value of 1.07 ± 0.05 nm obtained for *h*-BN/Rh(111).[11] Therefore, we suggest that the pores of the graphene nanomesh are of nearly the same size as for the *h*-BN nanomesh, but their lateral density is slightly higher.

In conclusion, graphene chemisorbs strongly on 4*d* TM surfaces such as Rh(111) and Ru(0001) and weakly on 5*d* TM surfaces such as Pt(111) and Ir(111) with the strength of covalent bonding growing in the series Pt-Ir-Rh-Ru. Strong chemical bonding in combination with lattice mismatch results in the formation of highly corrugated graphene nanomeshes on Rh(111) and Ru(0001). The structure of graphene nanomesh on Rh(111) is rather similar to that of the *h*-BN nanomesh.

We are grateful for the financial support by the Swedish Foundation for Strategic Research and the Swedish Research Council.

*alexeip@maxlab.lu.se

[1] J. V. Barth, G. Costantini, and K. Kern, Nature (London) **437**, 671 (2005).
[2] W. Chen and A. T. S. Wee, J. Phys. D **40**, 6287 (2007).
[3] A. T. N'Diaye, S. Bleikamp, P. J. Feibelman, and T. Michely, Phys. Rev. Lett. **97**, 215501 (2006).
[4] M. Corso, W. Auwärter, M. Muntwiler, A. Tamai, T. Greber, and J. Osterwalder, Science **303**, 217 (2004).
[5] A. Goriachko, Y. He, M. Knapp, H. Over, M. Corso, T. Brugger, S. Berner, J. Osterwalder, and T. Greber, Langmuir **23**, 2928 (2007).
[6] M. L. Ng, A. B. Preobrajenski, A. S. Vinogradov, and N. Mårtensson, Surf. Sci. **602**, 1250 (2008).
[7] H. Dil, J. Lobo-Checa, R. Laskowski, P. Blaha, S. Berner, J. Osterwalder, and T. Greber, Science **319**, 1824 (2008).
[8] R. Laskowski, P. Blaha, T. Gallauner, and K. Schwarz, Phys. Rev. Lett. **98**, 106802 (2007).
[9] R. Laskowski and P. Blaha, J. Phys.: Condens. Matter **20**, 064207 (2008).
[10] A. B. Preobrajenski, A. S. Vinogradov, M. L. Ng, E. Ćavar, R. Westerström, A. Mikkelsen, E. Lundgren, and N. Mårtensson, Phys. Rev. B **75**, 245412 (2007).
[11] A. B. Preobrajenski, M. A. Nesterov, M. L. Ng, A. S. Vinogradov, and N. Mårtensson, Chem. Phys. Lett. **446**, 119 (2007).
[12] S. Marchini, S. Günther, and J. Wintterlin, Phys. Rev. B **76**, 075429 (2007).
[13] P. A. Brühwiler, A. J. Maxwell, C. Puglia, A. Nilsson, S. Andersson, and N. Mårtensson, Phys. Rev. Lett. **74**, 614 (1995).
[14] O. Wessely, M. I. Katsnelson, and O. Eriksson, Phys. Rev. Lett. **94**, 167401 (2005).
[15] B. Lang, Surf. Sci. **53**, 317 (1975).
[16] Z. Hu, D. Ogletree, M. V. Hove, and G. Somorjai, Surf. Sci. **180**, 433 (1987).
[17] T. A. Land, T. Michely, R. Behm, J. Hemminger, and G. Comsa, Surf. Sci. **264**, 261 (1992).
[18] M. Sasaki, Y. Yamada, Y. Ogiwara, S. Yagyu, and S. Yamamoto, Phys. Rev. B **61**, 15653 (2000).
[19] H. Ueta, M. Saida, C. Nakai, Y. Yamada, M. Sasaki, and S. Yamamoto, Surf. Sci. **560**, 183 (2004).
[20] E. J. Mele and J. J. Ritsko, Phys. Rev. Lett. **43**, 68 (1979).
[21] X. Liu, T. Pichler, M. Knupfer, J. Fink, and H. Kataura, Phys. Rev. B **70**, 205405 (2004).
[22] A. B. Preobrajenski, S. A. Krasnikov, A. S. Vinogradov, M. L. Ng, T. Käämbre, A. A. Cafolla, and N. Mårtensson, Phys. Rev. B **77**, 085421 (2008).
[23] T. Aizawa, R. Souda, S. Otani, Y. Ishizawa, and C. Oshima, Phys. Rev. B **42**, 11469 (1990).
[24] A. Nagashima, N. Tejima, and C. Oshima, Phys. Rev. B **50**, 17487 (1994).
[25] K. C. Prince, I. Ulrych, M. Peloi, B. Ressel, V. Cháb, C. Crotti, and C. Comicioli, Phys. Rev. B **62**, 6866 (2000).
[26] S. Lizzit, L. Petaccia, A. Goldoni, R. Larciprete, P. Hofmann, and G. Zampieri, Phys. Rev. B **76**, 153408 (2007).
[27] Y. Gamo, A. Nagashima, M. Wakabayashi, M. Terai, and C. Oshima, Surf. Sci. **374**, 61 (1997).